This journal is (c) The Royal Society of Chemistry 2009

Metal-Organic Framework Structures – how closely are they related to Classical Inorganic Structures

Srinivasan Natarajan* and Partha Mahata

Electronic Supplementary Information

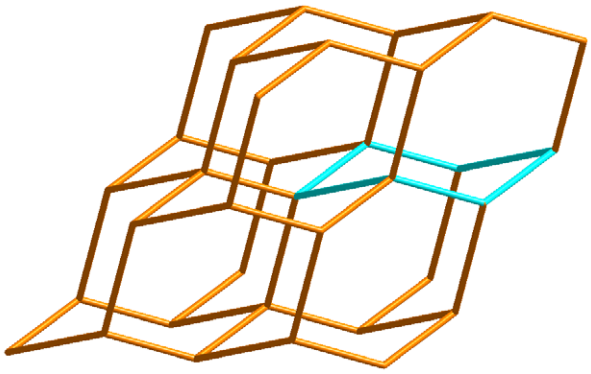

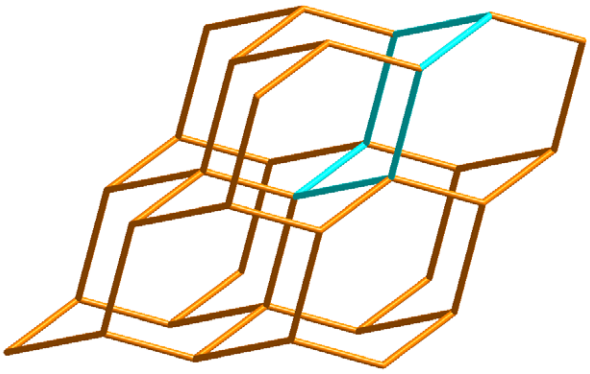

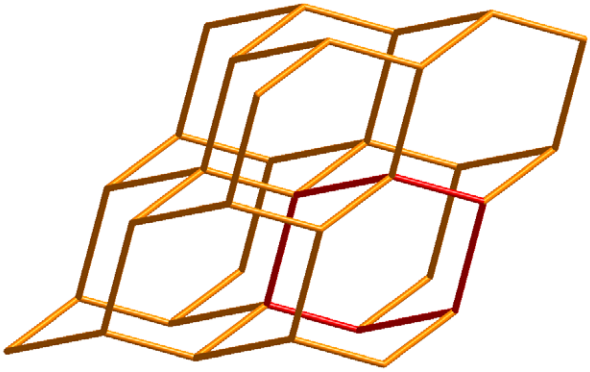

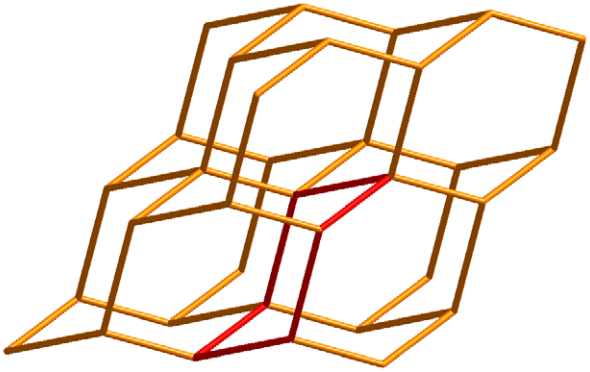

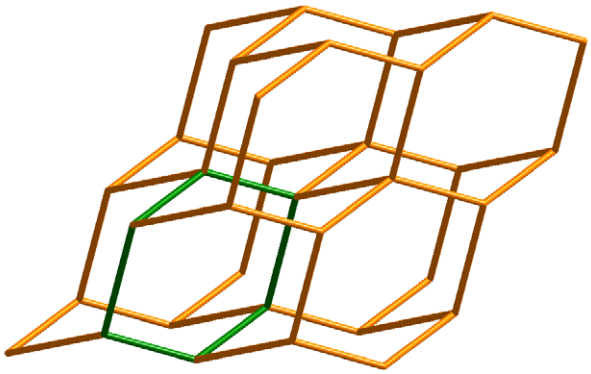

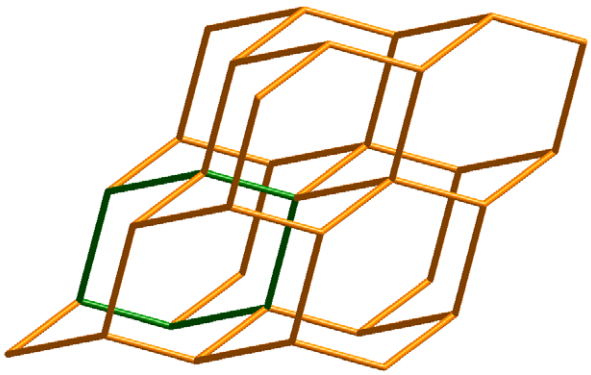

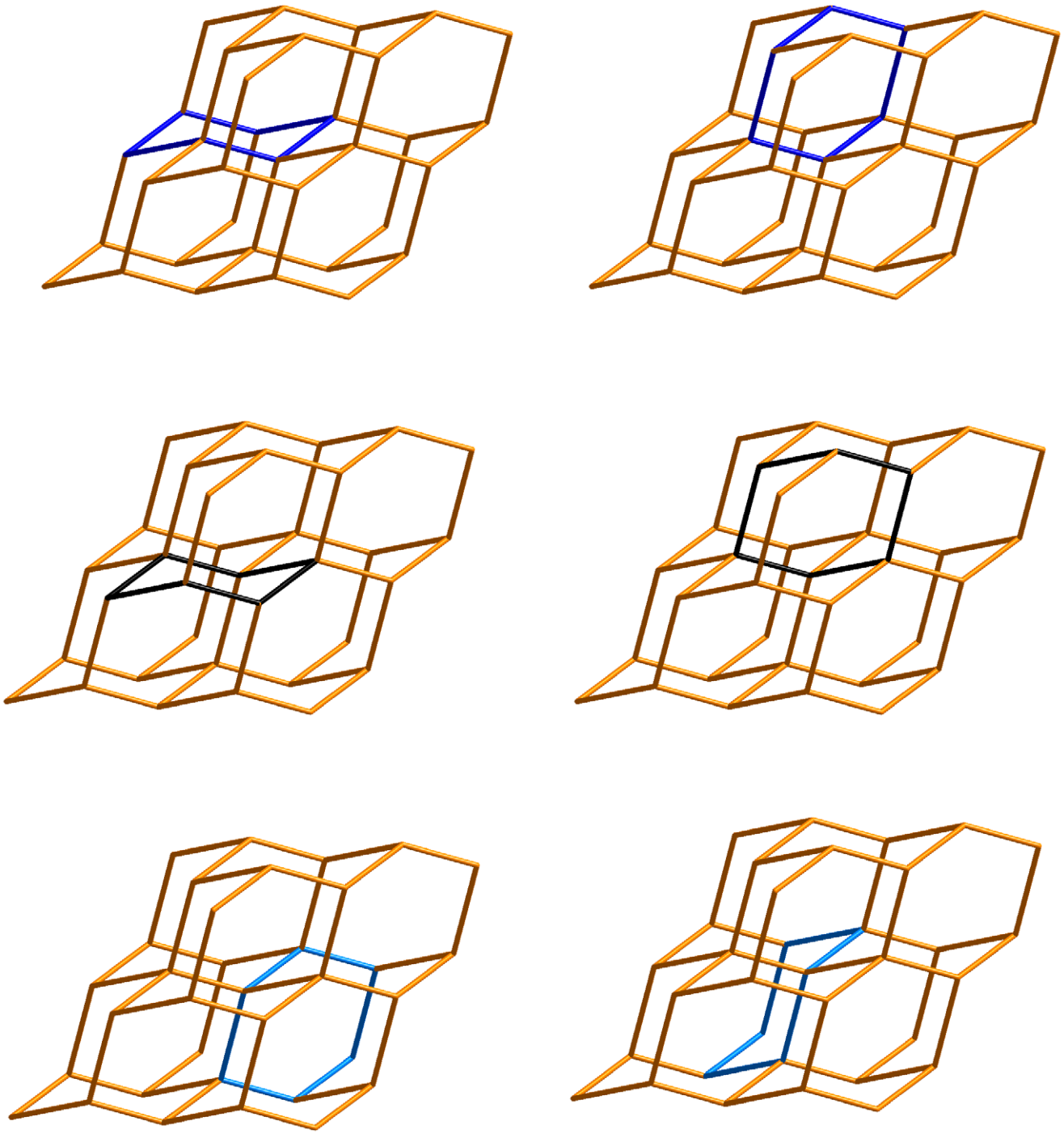

Figure S1: The figures illustrate 12 six-membered fundamental rings around a single node of the diamond net, which correspond to 2 rings per angle

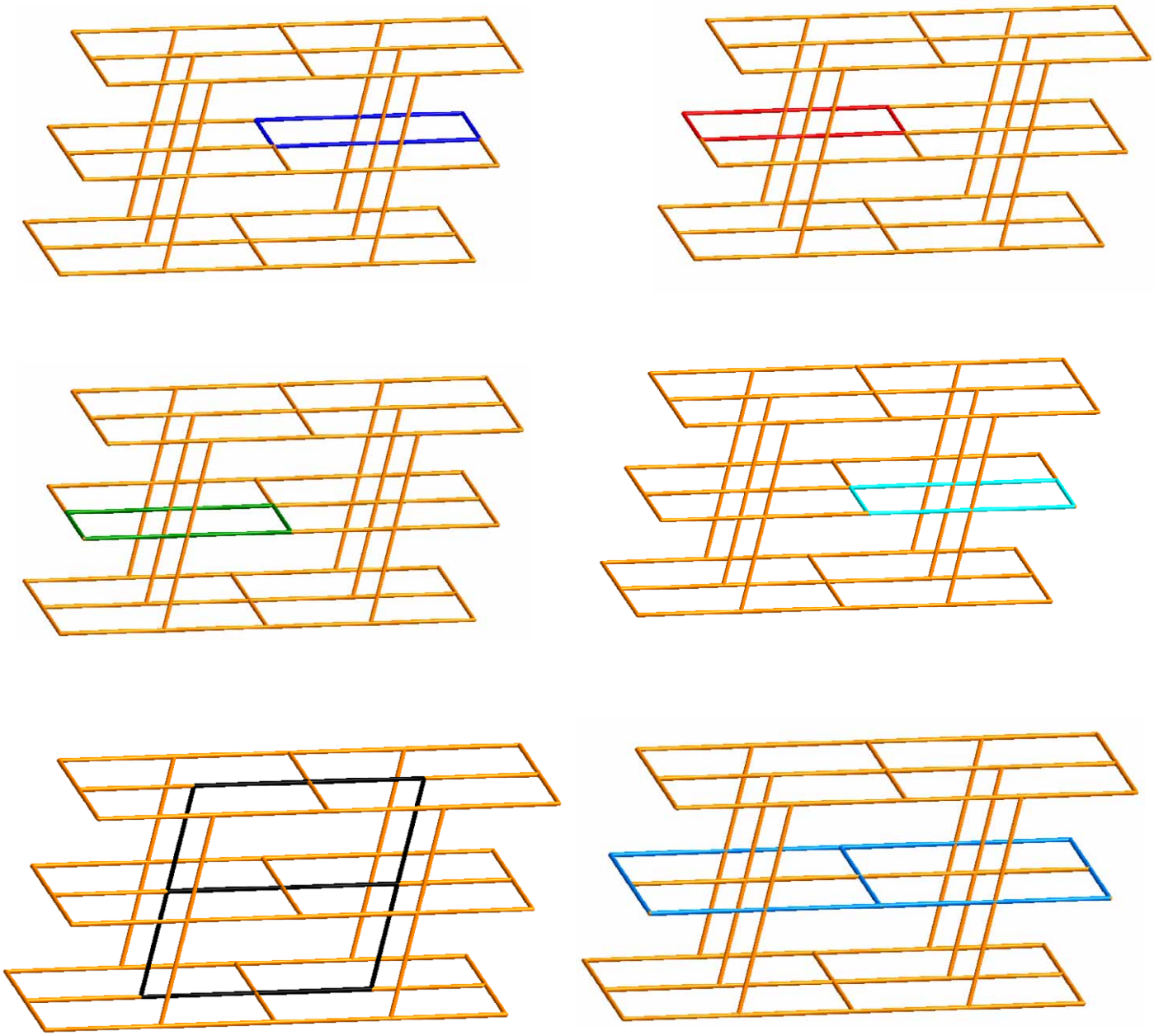

Figure S2: The figures illustrate the vertex symbol of the **cds** net. The figures show that around a single node of the **cds** net, four angles are associated with one 6-membered fundamental ring, one angle is associated with a two 6-membered fundamental rings and the other one is associated with two 8-membered shortest circuits. The eight membered shortest circuits are componed of two 6-membered fundamental rings.

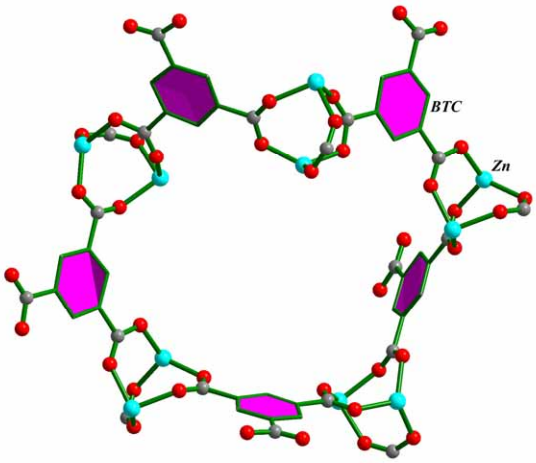

(a)

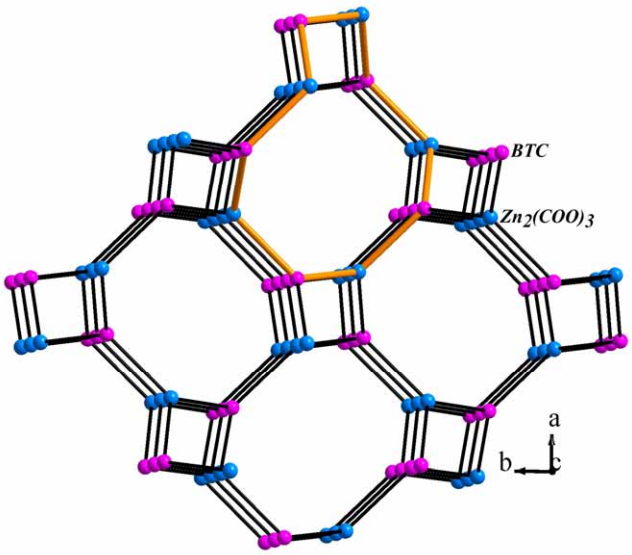

(b)

Figure S3: (a) The 10-membered fundamental ring of the **srs** net in $[Zn_2(BTC)(NO_3)]\cdot H_2O\cdot 5C_2H_5OH$ (BTC = 1,3,5-benzentricarboxylate), (b) The three-dimensional connectivity between the 3-connected $Zn_2(COO)_3$ units (light blue sphere) and the 3-connected BTC units (purple sphere) forming the **srs** net. One single 10-membered ring is highlighted by the orange bonds.

Reference: O. M. Yaghi, C. E. Davis, G. Li and H. Li, *J. Am. Chem. Soc.* 1997, **119**, 2861.

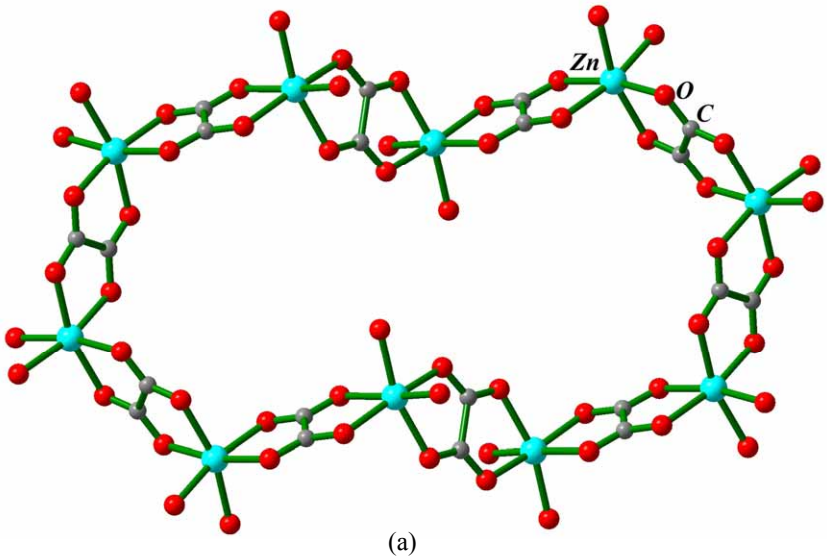

(a)

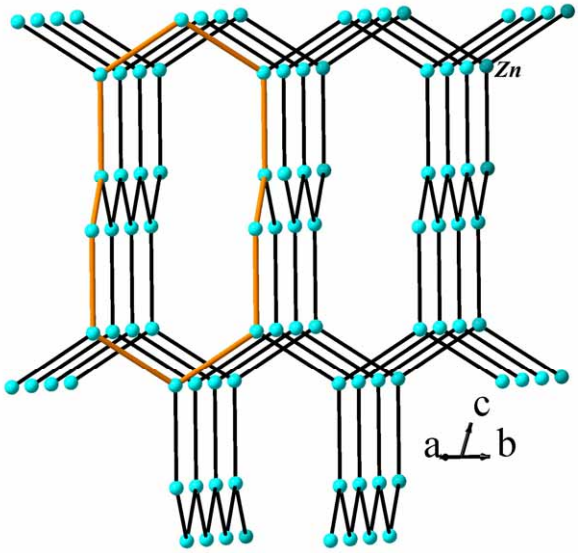

(b)

Figure S4: (a) The 10-membered fundamental ring (based on connectivity of the Zn^{+2} ion through oxalate linker) of the **ths** net in $[C_3H_7NH_3]_2[Zn_2(C_2O_4)_3]_2.3H_2O$, (b) The connectivity of 3-connected Zn^{+2} ions forming **ths** topology. One single 10-membered ring is highlighted by the orange bonds.

Reference: R. Vaidhyanathan, S. Natarajan, A. K. Cheetham and C. N. R. Rao, *Chem. Mater.* 1999, **11**, 3636.

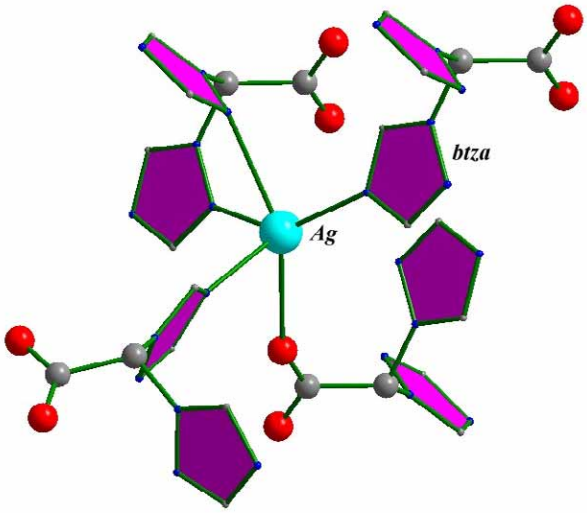

(a)

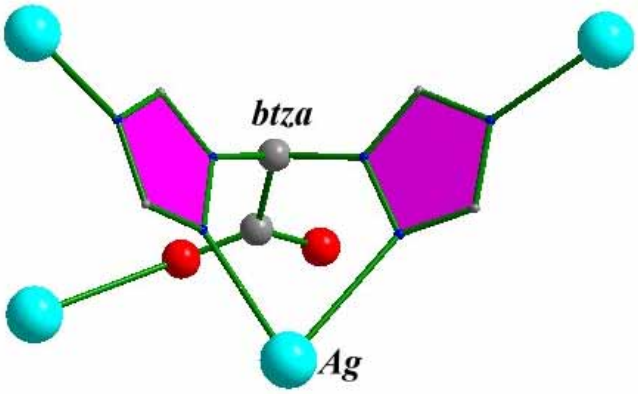

(b)

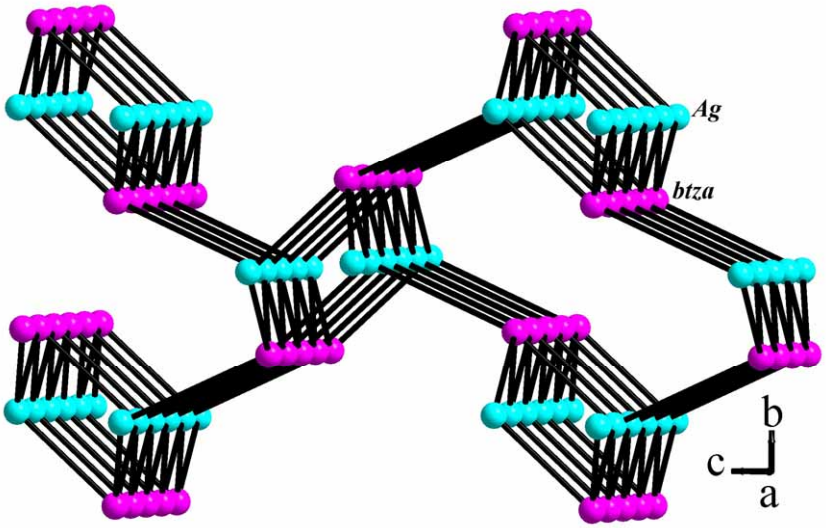

(c)

Figure S5: (a) Figure shows that Ag^{+} is connected with four btza unit in [Ag(btza)].CH_3OH (btza = bis(1,2,4-triazol-1-yl)acetate), (b) Figure shows that btza is connected with four Ag^{+} ions, (c) The connectivity between the Ag^{+} ions and btza units forming the **sra** net.

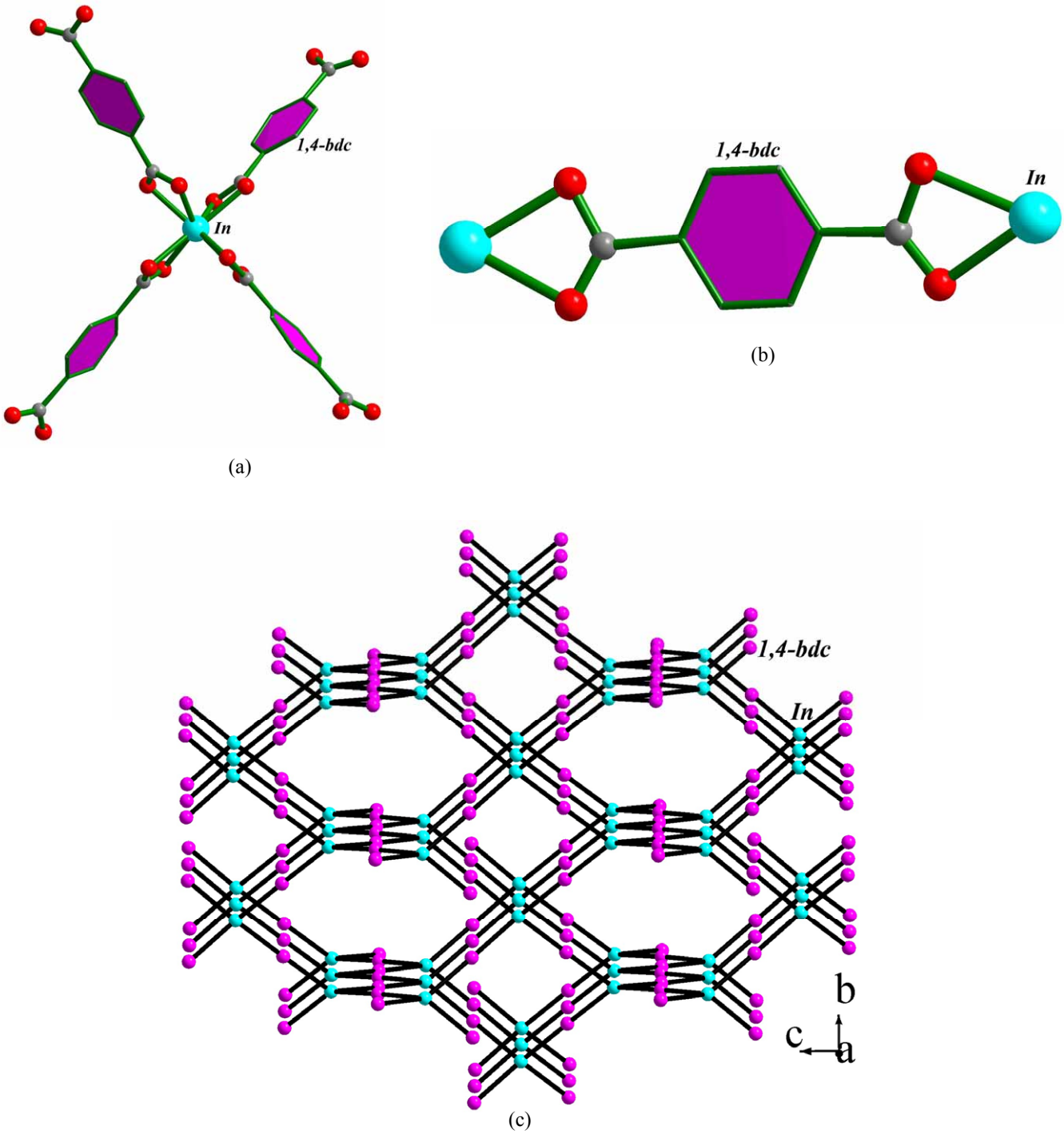

Figure S6: (a) Figure shows that In^{+3} ions is connected with four 1,4-bdc in $[InH(bdc)_2]$ (bdc = terephthalate) (b) Figure shows that 1,4-bdc is connected with two In^{+3} ions, (c) The connectivity between the In^{+3} ions and 1,4-bdc units forming the **qtz** (SiO_2) net.

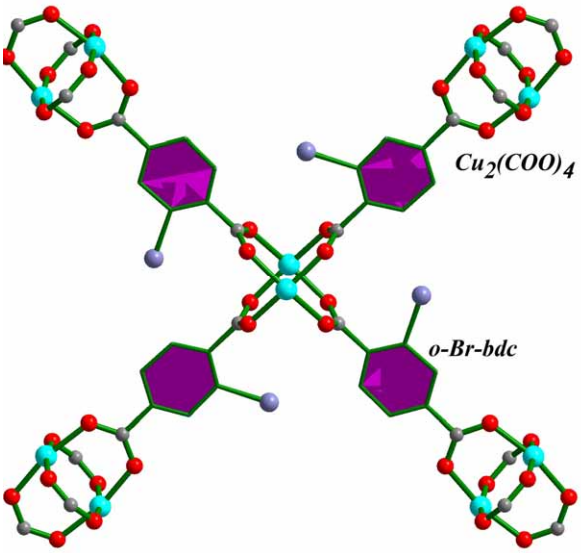

(a)

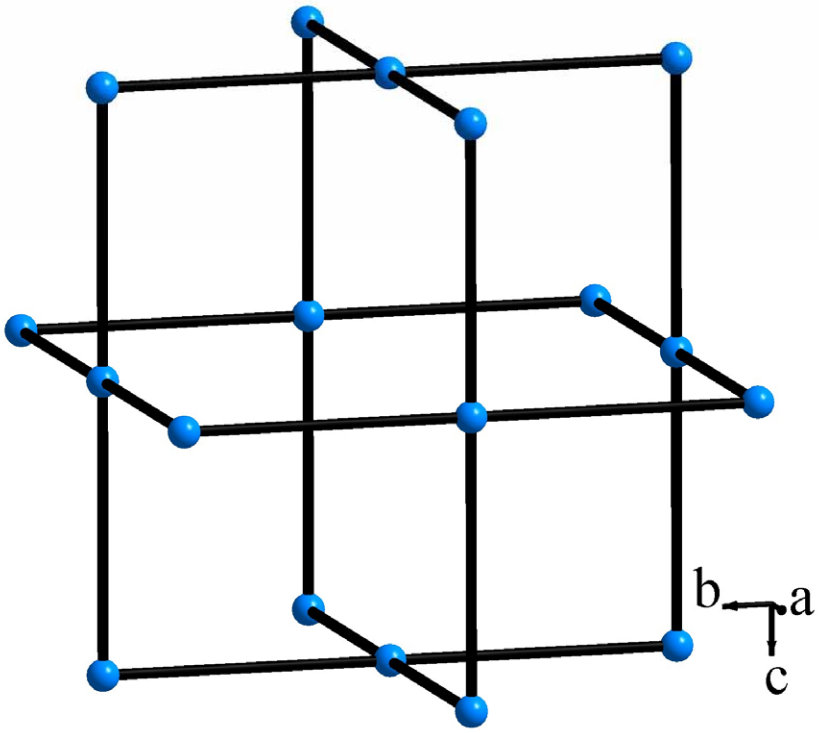

(b)

Figure S7: (a) The connectivity between the planar $Cu_2(COO)_4$ units and the 2-bromo-terephthalate linkers in $Cu_2\{o\text{-}Br\text{-}bdc\}_2(H_2O)_2].8DMF.2H_2O$ (o-Br-bdc = 2-bromo-terephthalate), (b) The connectivity of 4-connected $Cu_2(COO)_4$ units (light blue sphere) forming **nbo** topology.

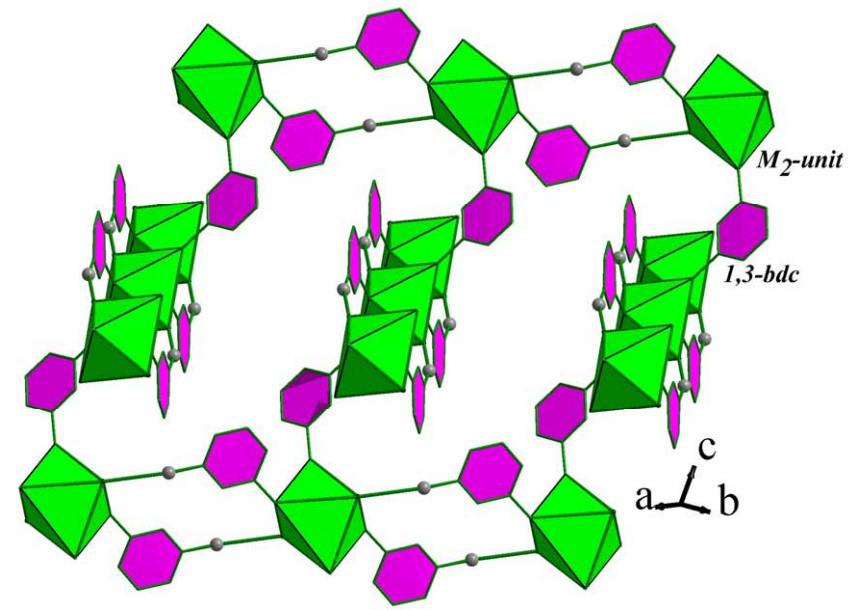

(a)

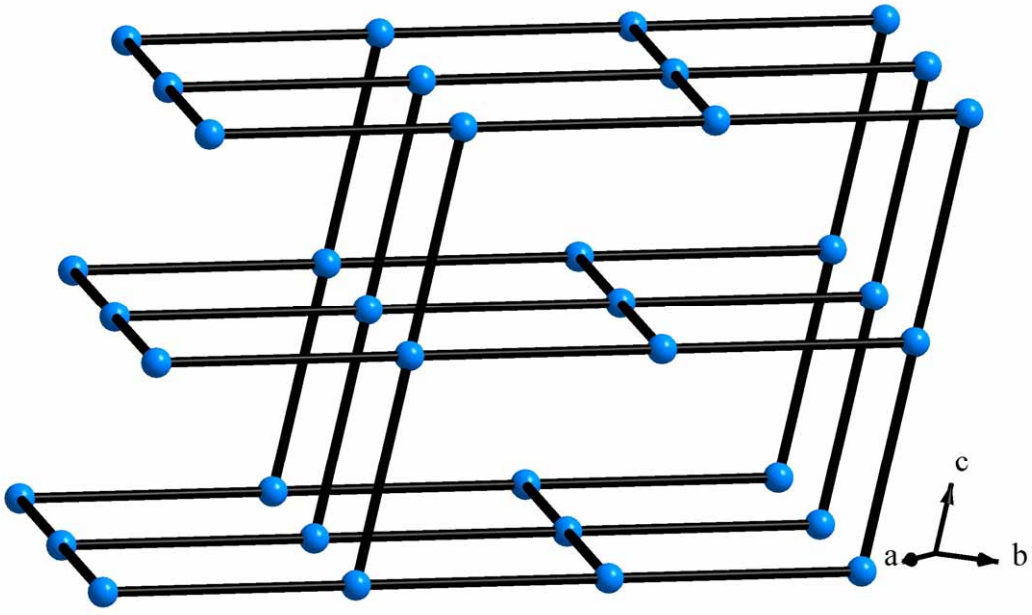

(b)

Figure S8: (a) Figure shows the three-dimensional structure of $[M_2(2,2'\text{-bipy})_2(1,3\text{-bdc})_3].2H_2O$ (M = Y, Gd, Dy; 1,3-bdc = isophthalate) through the connectivity of the M_2 unit and the isophthalate (1,3-bdc), (b) Figure shows the connectivity of the 4-connected M_2-units (light blue sphere) forming **cds** topology.

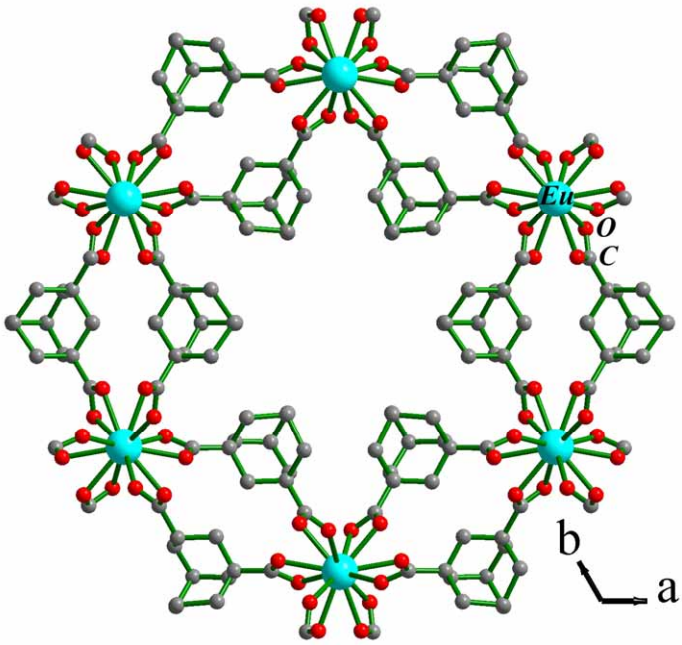

(a)

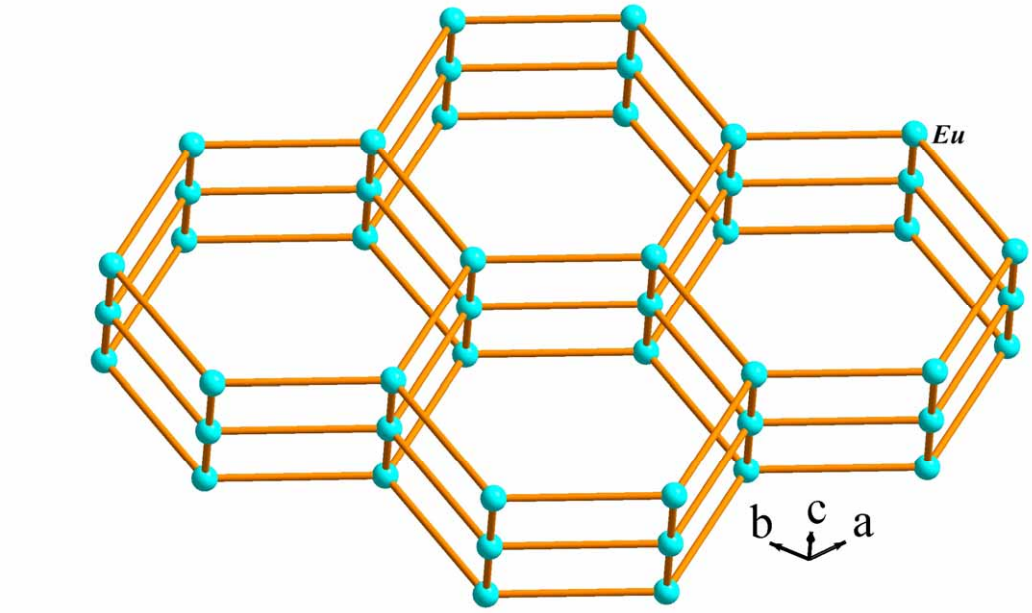

(b)

Figure S9: (a) Figure shows the connectivity between Eu^{+3} ions and the 1,3-adamanetanedicarboxylate in $[Eu_2\{C_{10}H_{14}(COO)_2\}_3]$, (b) Figure shows the connectivity of the five-connected Eu forming **bnn** net.

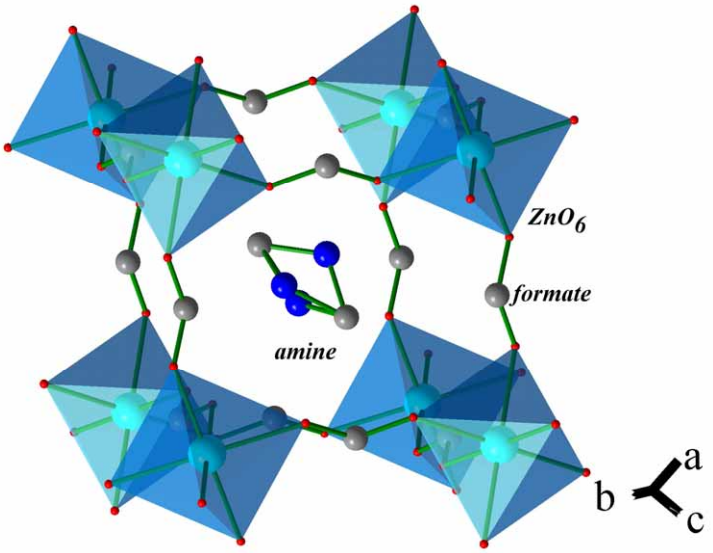

(a)

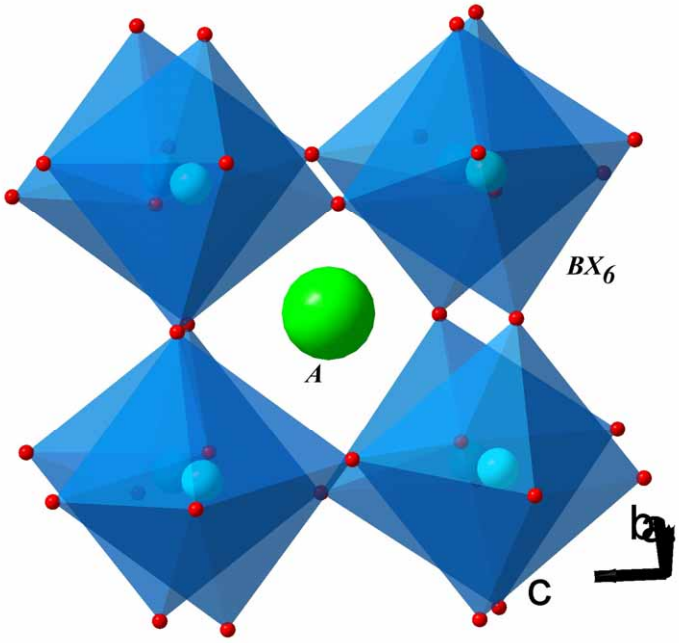

(b)

Figure S10: (a) Figure shows the connectivity between Zn^{+2} ions and $HCOO^{-}$ anions (formate) with $[(CH_3)_2NH_2]^{+}$ ion at the middle forming perovskite structure in $[(CH_3)_2NH_2]Zn(HCOO)_3$, (b) The ideal perovskite structure with the general formula of ABX_3. Note the similarity between the two structures

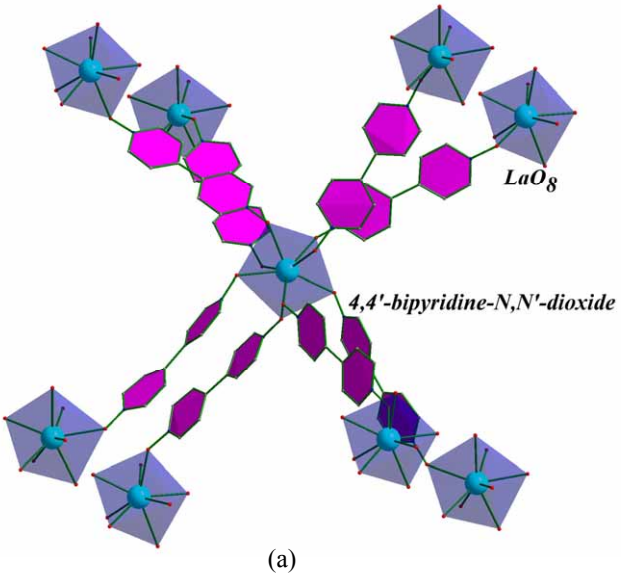

(a)

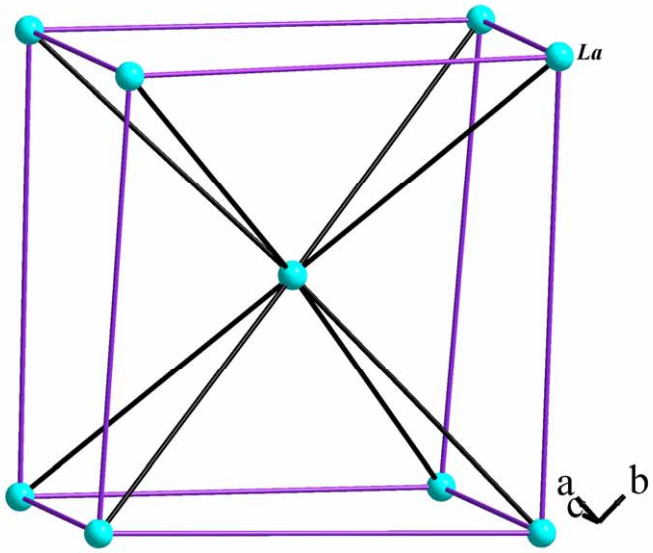

(b)

Figure S11: (a) Figure shows La^{+3} ion is connected with eight other La^{+3} ions through 4,4'-bipyridine-N, N'-dioxide bridging ligand in $[La(4,4'\text{-bipyridine-N, N'-dioxide})_4].(CF_3SO_3)_3.4.2CH_3OH$, (b) Figure shows the connectivity of the 8-connected La^{+3} ions forming **bcu** topology. The elementary cell edge of the **bcu** structure is shown by violet line.

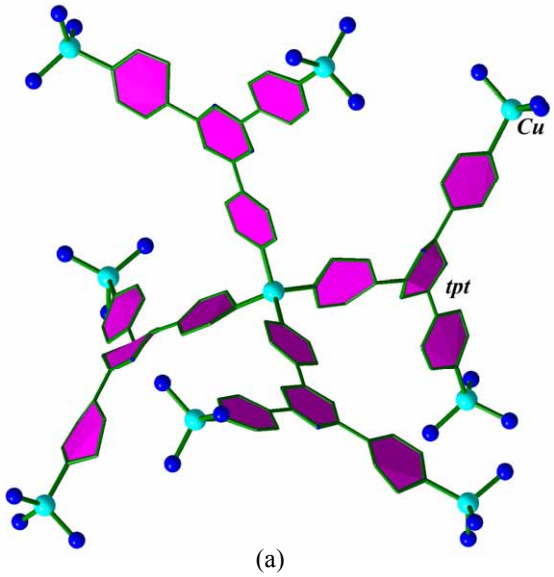

(a)

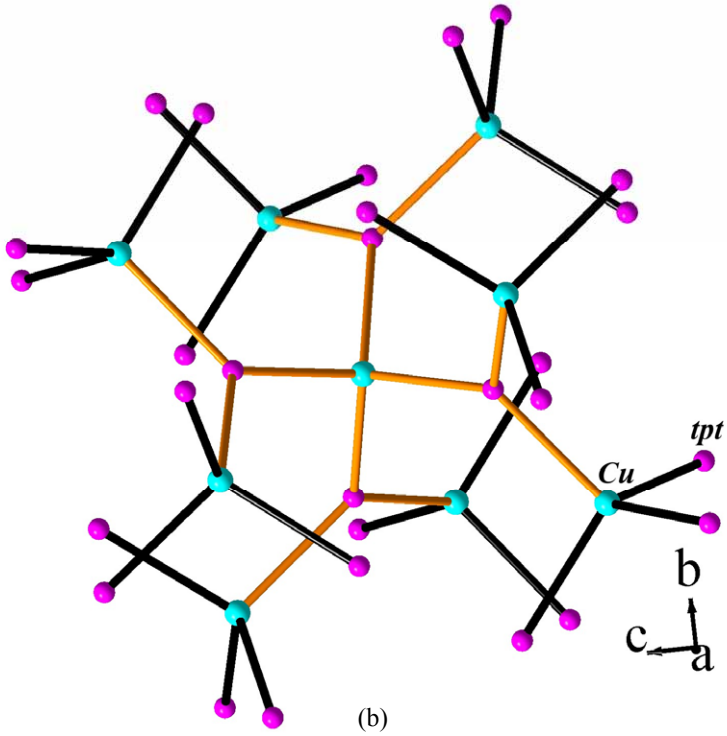

(b)

Figure S12: (a) Figure shows the connectivity between the Cu^{+} (tetrahedral) ions and the 3-connected TPT (trigonal) ligands in $[Cu_3(tpt)_4](BF_4).(tpt)_{2/3}.5H_2O$, (b) The connectivity between 4-connected Cu^{+} ions (cyan sphere) and 3-connected TPT ligand (purple sphere) forming C_3N_4 net. The figure a is highlighted by orange bonds based on the connectivity of the nodal positions.

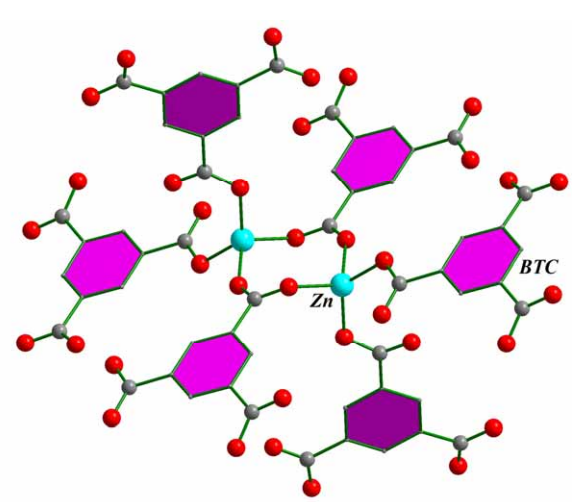

(a)

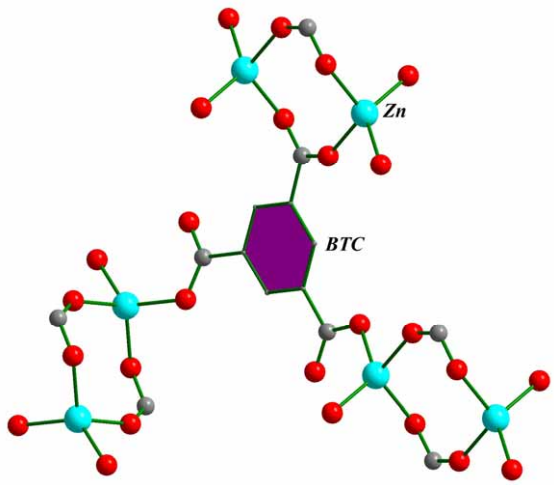

(b)

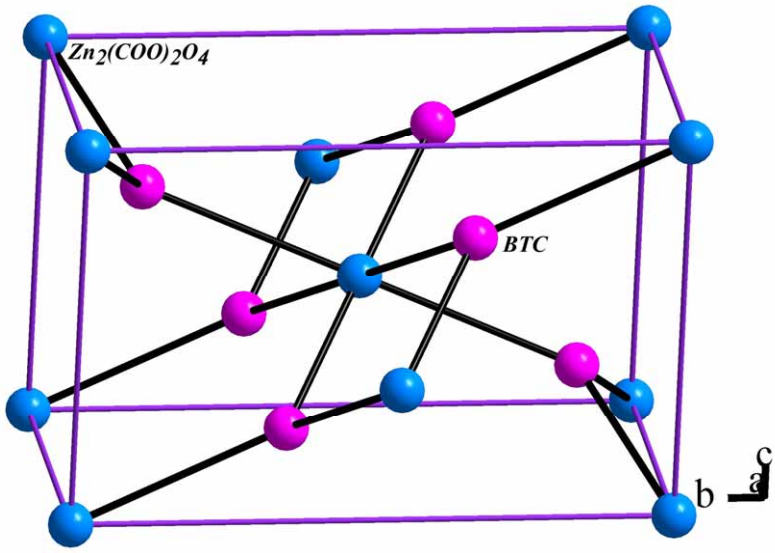

(c)

Figure S13: (a) Figure shows $Zn_2(COO)_2O_4$ unit is connected with six 1,3,5-benzenetricarboxylate and act as octahedral node in [Zn(1,3,5-benzenetricarboxylate)].$NH_2(CH_3)_2$.DMF, (b) Figure shows 1,3,5-benzenetricarboxylate unit is connected with three $Zn_2(COO)_2O_4$ units, (c) The connectivity between the $Zn_2(COO)_2O_4$ unit and the 1,3,5-benzenetricarboxylate forming **rtl** topology. The elementary cell edge of the rutile structure is shown by violet line.

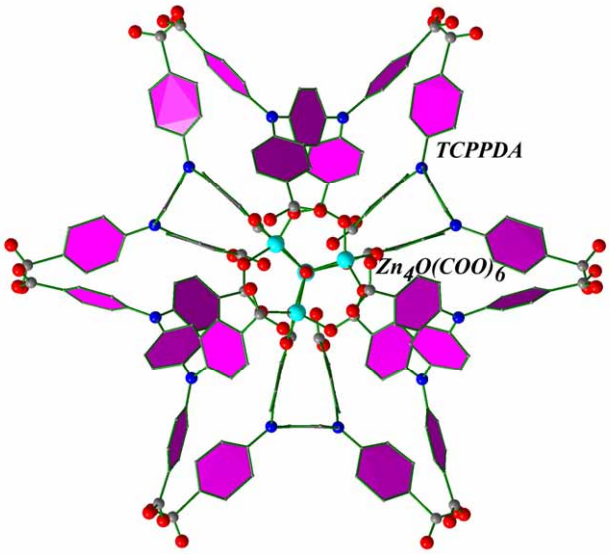

(a)

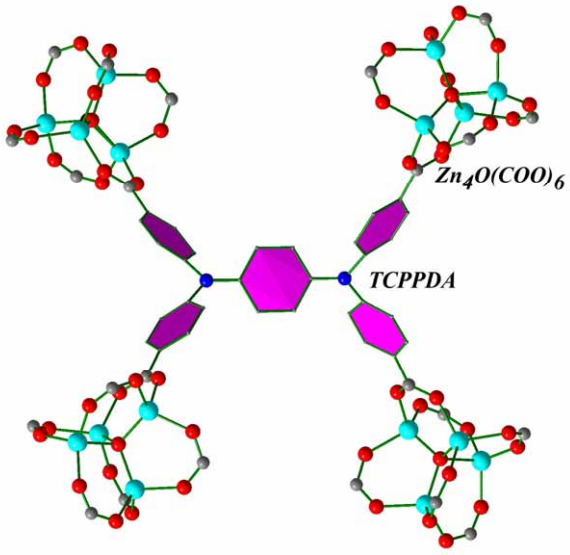

(b)

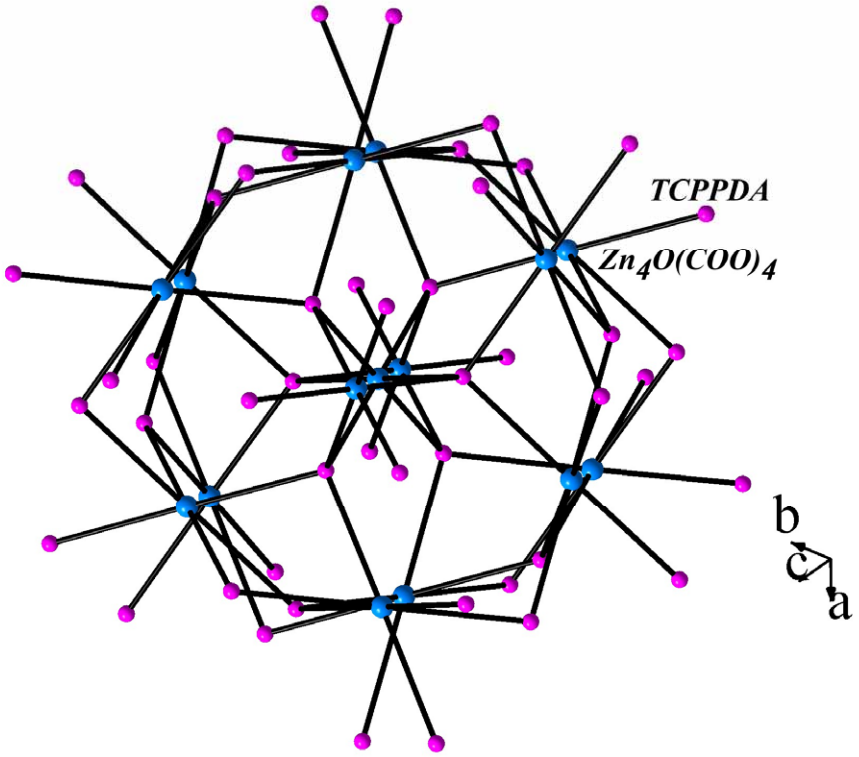

(c)

Figure S14: (a) Figure shows $Zn_4O(COO)_6$ unit is connected with six TCPPDA units and acts as octahedral node in [$Zn_4O(D_2$-tcppda).DMF.H_2O (DMF = N, N'-dimethylformamide, D_2-tcppda = N, N, N', N'-tetrakis(4-carboxyphenyl)-1,4-phenylenediamine with D_2 symmetry), (b) Figure shows TCPPDA unit is connected with four $Zn_4O(COO)_6$ units and acts as tetrahedral node, (c) The connectivity between the six connected $Zn_4O(COO)_6$ units and four connected D2-TCPPDA forming **cor** net.

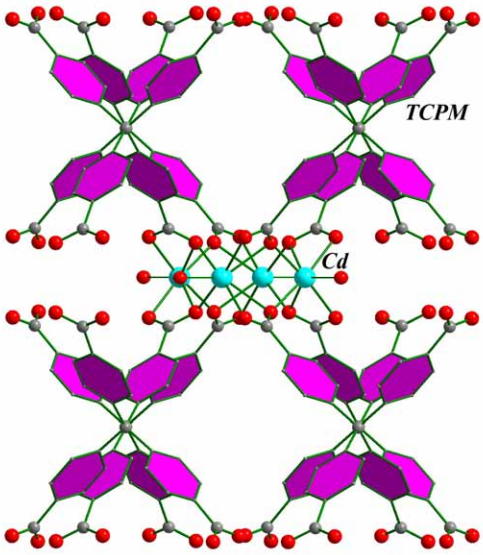

(a)

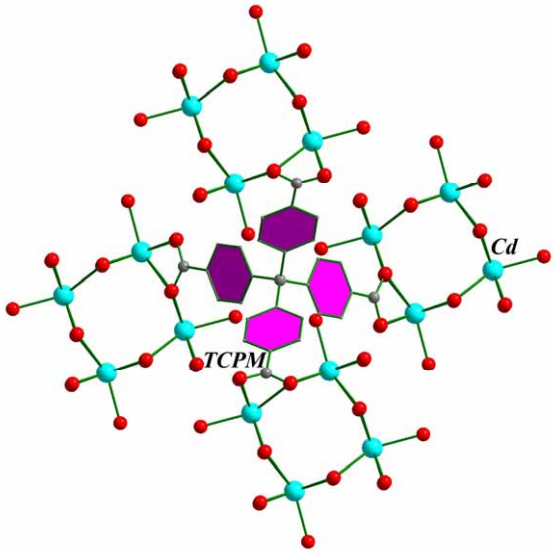

(b)

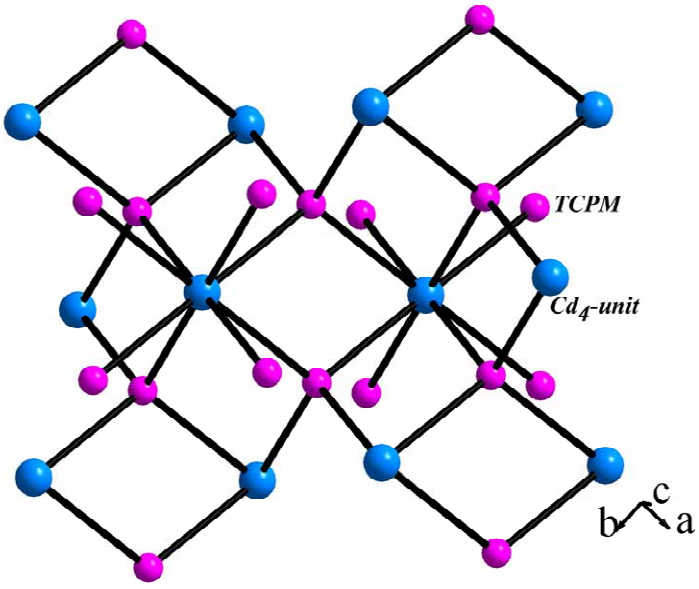

(c)

Figure S15: (a) Figure shows Cd_4 cluster is connected with eight TCPM ligands and acts as a cubic node in $[Cd_4(TCPM)_2(DMF)_4].4DMF.4H_2O$ (TCPM = tetrakis-(4-carboxyphenyl) methane), (b) TCPM ligand is connected four Cd_4 clusters and acts as tetrahedral node, (b) The connectivity between the 8-connected Cd_4 and the four connected TCPM ligands to form fluorite net.